Optimizing and Enhancing Piezoelectric Energy Harvesting Devices

Chaymae Amri[1*], *Khawla* Gaouzi[1], *Abdelilah* Jilbab[1], *My Hachem* el Yousfi Alaoui[1], and *Lahcen* Azrar[2]

[1]Centre STIS, E2SN, Team ENSAM, Mohammed V University in Rabat, Morocco
[2]Centre STIS, M2CS, Team ENSAM, Mohammed V University in Rabat, Morocco

Abstract. This paper presents a study on energy harvesting from very low excitation frequencies 0.7 Hz, 0.9 Hz, and 1 Hz simulating a pedestrian's walking motion using a piezoelectric energy generator. This generator is based on a cantilever beam model with a concentrated mass at its end. A more complex model was considered, incorporating a test mass of 1 g after various manual mass adjustments. Upon validation through modelling and simulation, the energy harvesting system produced power recoveries of 68 mW, 98 mW, and 196 mW for frequencies of 1 Hz, 0.9 Hz, and 0.7 Hz, respectively. The system was further optimized electrically using the Synchronized Switch Harvesting on Inductor (SSHI) method, which inverts the piezoelectric voltage, increasing the amplitude of the crenels and enhancing the device's efficiency. This optimization resulted in harvested power increases to 139 mW, 190.3 mW, and 396 mW at the respective frequencies. Overall, power recovery improved by 50% following the electrical optimization. These results demonstrate the potential to enhance and scale up the system for harvesting and storing energy in batteries through a larger-scale prototype. This technology provides a renewable and unlimited energy source, particularly useful for biomedical sensors with strict energy requirements.

1 Introduction

The energy crisis of the 2000s has greatly motivated the exploration of clean energy sources, such as vibrational energy, bioenergy and thermal energy, as substitutes for traditional fossil fuels [1]. Vibrational energy recovery represents a promising avenue in the field of renewable energy. It involves capturing the energy produced by vibrations in various environments, particularly mechanical movements, and converting it into usable energy. Various mechanisms have been developed to recover energy from human movements, including electromagnetic, piezoelectric and triboelectric systems [2]. Among vibratory energy recovery techniques, the piezoelectric stands out. Piezoelectric exploited the phenomenon whereby certain materials generate an electrical charge in response to mechanical stress, such as pressure or vibration. Of the energy sources available in human movement, step energy is recognized as the most important [3]. Recovering energy from human walking steps using piezoelectric devices represents an innovative and sustainable solution to the problem of powering biomedical sensors. Piezoelectric devices convert mechanical energy, generated by the pressure of footsteps, into electrical energy. This technology can provide a renewable and inexhaustible source of energy, essential for biomedical sensors often constrained by battery

* Corresponding author: chaymae_amri@um5.ac.ma

© The Authors, published by EDP Sciences. This is an open access article distributed under the terms of the Creative Commons Attribution License 4.0 (https://creativecommons.org/licenses/by/4.0/).

limitations. To optimize this system, precise manual adjustments and electrical optimizations are required to maximize energy efficiency. For example, configuring piezoelectric devices and improving energy storage and transfer circuits can significantly increase power output. By applying this concept to high-traffic environments such as schools, it is possible to develop a prototype piezoelectric mat. This prototype could harness students walking to generate electricity, offering a practical and promising solution. By combining these approaches, we can not only solve the challenges of powering biomedical sensors, but also pave the way for innovative applications of piezoelectric technology in our everyday lives.
A variety of innovative approaches have been explored to harvest kinetic energy from human motion. One study integrated a PVDF sole and a thunderous PZT unimorph into shoes, achieving average power outputs of 1.1 mW and 1.8 mW, respectively [4]. Flexible wearable devices have been developed for kinetic energy harvesting, including an analytical model for a piezoelectric energy recuperator placed on the knee. This model, validated by a prototype, accurately predicted power generation, demonstrating that the device could produce 161 µW at 5 mph, sufficient to power a 35µA load [5]. Another notable development is a piezoelectric device with a two-stage force-reinforcement mechanism, designed to capture energy from walking. Tests revealed an average power of 34.3 mW and a maximum of 110.2 mW under a dynamic force of 500 N at 3 Hz. At 2 Hz and 1.0 Hz, the average power outputs were 23.9 mW and 11.0 mW, with peak power measurements of 65.8 mW and 31.7 mW. Numerical simulations suggested an average power of 12.8 mW and a maximum of 204.7 mW at a walking speed of 3.5 mph for an 84 kg male [6].

Almouahed et al. [7] proposed an instrumented knee replacement with four piezoelectric transducers embedded in the knee implant's tibial plateau. In 2016, it was shown that this design could generate up to 4.276 mW of average power at an optimal resistive load of 50 kΩ, optimized by transducer position, material, and size [8]. Using a frequency up-conversion mechanism, a knee-worn device produced 2.06 mW of power during typical walking. Later that year, this group enhanced the device by replacing the mechanical buckling mechanism with a magnetic one, increasing the output to 5.8 mW [9]. Despite these advancements, the electromagnetic shoe generator faced criticism for its bulkiness and long stroke, potentially causing discomfort for users. A curved PZT bimorph with a metal middle plate mounted in a heel produced an average power of 8.4 mW at an optimal resistance of 500 kΩ at 0.9 Hz. The highest average output recorded was 11.3 mW at a compression frequency of 1.07 Hz, resulting in a power density of 10.55 mW/cm³ [10]. These pioneering studies have significantly advanced our understanding and inspired further research into energy recovery from human motion. However, most piezoelectric energy harvesters still produce low power outputs, typically in the milliwatt range or less, due to low excitation levels and frequencies [11]. Based on our problem and recommendations from the literature, we will improve our energy recuperated by making manual adjustments and electrically optimizing the system to obtain the most efficient solution. A promising concept is to develop a prototype mat equipped with piezoelectric devices in high-traffic areas, such as schools, to exploit student walking and generate electricity. This paper, presents a modeling and simulation study, starting with a single piezoelectric element to recover energy from human walking, where the vibration frequency is very low. Walking has proven to be the most practical energy source [12], due to its relatively low frequency, ideal for piezoelectric devices. Our study, focusing on the specific conditions of human footsteps, aims to provide valuable insights for the development of efficient energy harvesting technologies. These results could guide the design of prototype mats with multiple piezoelectric devices, opening up new possibilities for the practical integration of this technology and contributing to the advancement of renewable energies.

In this paper, we will study the design of the energy generator structure under specific conditions. We carried out modeling and simulation of our system to assess its ability to efficiently capture the energy generated by human footsteps. Our system was then improved using the SSHI optimization method. This method will enable us to understand how to optimize the configuration of piezoelectric devices to maximize energy recovery in a concrete setting.

2 Power generator structure design

The design of the power harvester considers two essential parameters: the mass of the system and the excitation frequency. The objective of the optimization is to reduce the excitation frequency and increase the recovered energy. The proposed power generator uses a cantilever bimorph piezoelectric beam of rectangular shape, with a mass concentrated under the tip. Figure 1 schematically illustrates a cantilever beam under a harmonic excitation $f(x,t)$ [13]. We assume that Young's modulus E, moment of inertia I and cross-sectional area A are constant along the beam axis. The majority of studies are based on the cantilever design using Lead Zirconate Titanate (PZT) as the piezoelectric component [14] [15]. The square proof mass [16] at the tip helps adjust the resonant frequency. When an input acceleration is applied to the structure, the mass converts the input acceleration into a force. This will cause the beam to bend, which in turn results in distributed stress along the beam. Displacement of the beam causes compression or tension of the piezoelectric layer. This creates a charge accumulation due to the piezoelectric effect. The basic formula for a piezoelectric material in the stress-charge formulation are as follows:

$$T = [c]\,S - [e]^T D \tag{1}$$

$$G = [e]\,S - [\epsilon^S]\,D \tag{2}$$

where T is the stress field, c is the complacency tensor, S is the strain field, e is the piezoelectric stress coefficient tensor, D is the electric field, G is the electric displacement field and ϵ^S is the permittivity tensor at constant or zero strain.

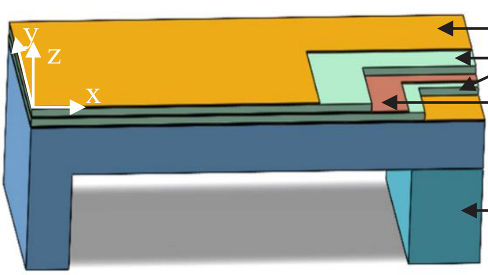

Fig. 1. Structure of a piezoelectric vibration energy harvester.

The proposed power generator is modeled using Euler-Bernoulli beam theory. This approach assumes that rotation of the differential element is negligible compared to translation, and that angular distortion due to shear is insignificant compared to bending deformation [17].

$$E\,I\,\frac{\partial^4 u(x,t)}{\partial x^4} + m\,\frac{\partial^2 u(x,t)}{\partial t^2} + b\,\frac{\partial u(x,t)}{\partial t} = f(x,t) \tag{3}$$

Where $m = \rho A$ is the linear density of the beam, ρ is the density, b is the damping factor per unit length, $f(x,t)$ is the force per unit length and $u(x,t)$ designates the transverse displacement of the beam point which has distance x from the origin.

2.1 Electrical system modelling

The lumped circuit model of the piezoelectric beam, considered, is shown in the Figure 2. The sinusoidal voltage source in series with C_p is used to depict the vibrating piezoelectric beam [18]. The structure is animated by a sinusoidal motion of constant amplitude u_M. The equation is obtained by directly connecting a resistor across the piezoelectric elements.

$$I_p = \frac{V}{R} = \alpha \, \dot{u} - C_p \, \dot{V} \tag{4}$$

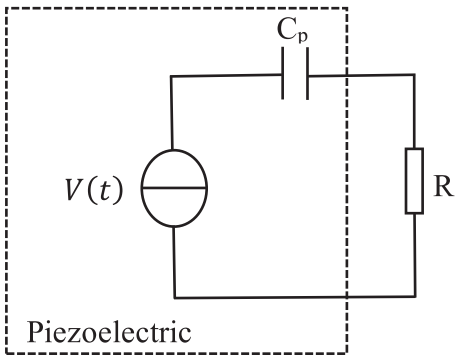

Fig. 2. Lumped circuit model of the piezoelectric beam.

In the frequency domain, equation (5) represents the voltage on the piezoelectric elements as a function of their displacement, the load resistance and the parameters α, namely the overall piezoelectric coefficient, and C_p the overall force factor and equivalent capacitance of the piezoelectric element. Displacement is represented by u, while the beam's natural frequency is ω.

$$\tilde{V} = \frac{\alpha \, R}{1 + j\omega \, C_p \, R} \, j\omega \, \tilde{u} \tag{5}$$

Recovered power is the energy dissipated in the load resistor. Its value is expressed by equation (6). The power admits a maximum P_{max} equation (7) for a given resistance R_{opt} equation (8) for a given pulsation.

$$P = \frac{\tilde{V}\tilde{V}}{2R} = \frac{1}{2} \, \frac{\alpha \;\, R}{1 + (\omega \; R \; C_p)^2} \, \omega^2 \, u_M^2 \tag{6}$$

The parameters of the circuit model, i.e.V, I_P and C_p, are determined with the piezoelectric device and the vibration source. In other words, they are not related to the resistive load. Thus, the optimum load resistance and corresponding maximum output power are as follows:

$$P_{max} = \frac{\alpha^2}{4 \, C_p} \, \omega \, u_M^2 \tag{7}$$

$$R_{opt} = \frac{1}{\omega \, C_p} \tag{8}$$

From the above equations, it can be seen that the output voltage and power are influenced by various parameters. All these parameters play a crucial role in the design of the piezoelectric power generator, as does the amplitude of the sinusoidal motion, which plays an interesting role: each time the amplitude of the motion increases, the power recovery increases.

2.2 Energy recovery system modelling

This study uses a piezoelectric bender, when bending it generates an electrical potential. It represents a bimorph piezoelectric beam with a rectangular cross-section. The piezoelectric bender at the left end is attached to a vibrating object, which drives the motion. This block forms a mechanical rotation port that rotates without constraint, without the need for torque. The piezoelectric bender has a right-hand end which is connected to an additional mass. Due to the elasticity, mass and inertia of the piezoelectric bender, the movement of the right-hand end is not synchronous with that of the left-hand end. Figure 3 shows the energy harvesting system proposed, consisting of a piezoelectric bender, a rectifier, a DC-DC converter, a battery and a load. The energy recovered will be used to power a load or stored in a battery.

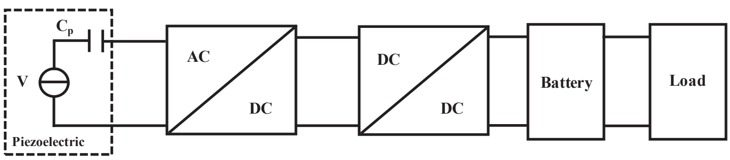

Fig. 3. Proposed energy recovery system architecture.

The full-wave rectifier transforms the alternating current generated by the piezoelectric bender into direct current, consisting of four diodes and a capacitor acting as a filter to smooth the DC voltage. The step-down converter to transfer maximum power to the load regulates the voltage. This optimized voltage is then applied to the battery to ensure efficient charging. Walking frequency generally varies between 0.7 Hz and 1.2 Hz, depending on the speed of movement and body morphology [19] [20]. In this study, three different excitation frequencies: 0.7 Hz, 0.9 Hz, and 1 Hz will be investigated. The results obtained for each frequency will then be analysed to evaluate the system's response to each respective frequency.
The piezoelectric device is subjected to a sinusoidal force represented by the following function:

$$F = u_M \sin(\omega\, t) \qquad (9)$$

where u_M is the amplitude of the applied force and $\omega = 2\pi f_0$ is the angular frequency, with f being the total frequency of the system, which is 185 Hz. Less than 200Hz, which keeps us in the very low frequency range [21].

3 Simulation and results

Simulations were carried out using MATLAB/Simulink software to test the proposed model of the piezoelectric vibration energy harvesting. In the next section, the exerted force is equivalent to the force applied by a person weighing 80 kg. Many tests have been explored to optimize and enhance the performance of the piezoelectric energy harvesting devices. The first subsection concerns the manual setting, where the mass m has been varied with different values of excitation frequencies: 1 Hz, 0.9 Hz, and 0.7Hz. proposing the use of Schottky diodes in the rectifier stage. The second part concerns the electrical optimization of the energy harvesting system. The SSHI (Synchronized Switch Harvesting on Inductor) method was studied, proposing the use of Schottky diodes in the rectifier stage.

 https://doi.org/10.1051/e3sconf/202560100019

3.1 Manual setting

The resonant frequency f_0 of the energy recuperator can be adjusted by modifying the stiffness, or the mass m, which corresponds to equation (10) [22]. In our case, we are interested in modifying the mass, where l is the piezoelectric length.

$$2\pi f_0 = 1.885^2 \sqrt{\frac{EI}{ml^3}} \tag{10}$$

To begin, a manual adjustment will be made to the energy recovery system by assigning three distinct values to the mass: 1.2 g, 1 g and 0.8 g. The system's response to these different mass values will then be examined to analyze its behavior and improve its performance. For instance, an excitation frequency of 0.7 Hz will be considered.

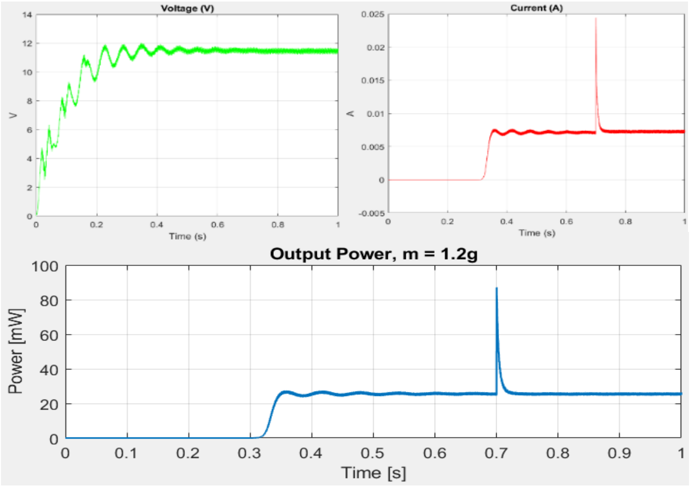

Fig. 4. Voltage, current and power recovered from a 1.2g mass.

Figure 4 shows the response of the system is the case where the mass value is 1.2 g. In this situation, the piezoelectric device has a rectified output voltage of 11.70 V, while the current is 0.0055 A. The system produces a power of 25 mW, but there is a very significant delay in its response, reaching 0.33 s. This considerable delay is mainly caused by the slowness of the current response. This delay reduces the overall efficiency of the energy recovery system compared with other ground configurations.

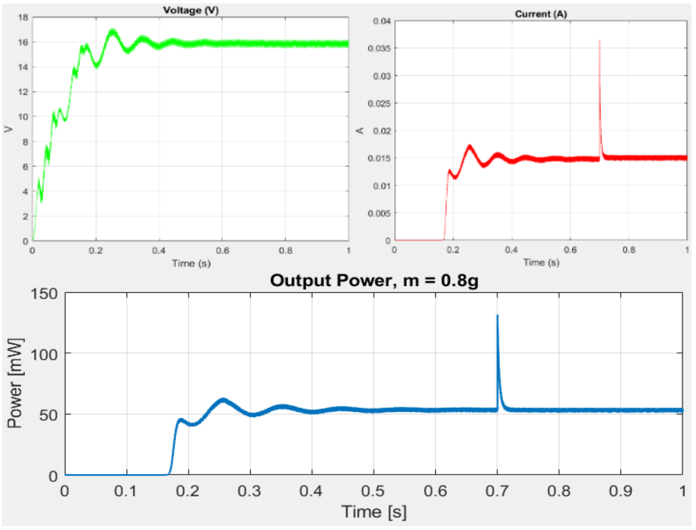

Fig. 5. Voltage, current and power recovered from a 0.8g mass.

Figure 5 illustrates the case where the mass is 0.8 g. The voltage reaches a significant value of 16 V, while the current is 0.015 A. It is observed that the power reaches 52 mW, although the system shows a slight response delay, reaching nearly 0.2 s. This delay is primarily due to the lag in the current's response.

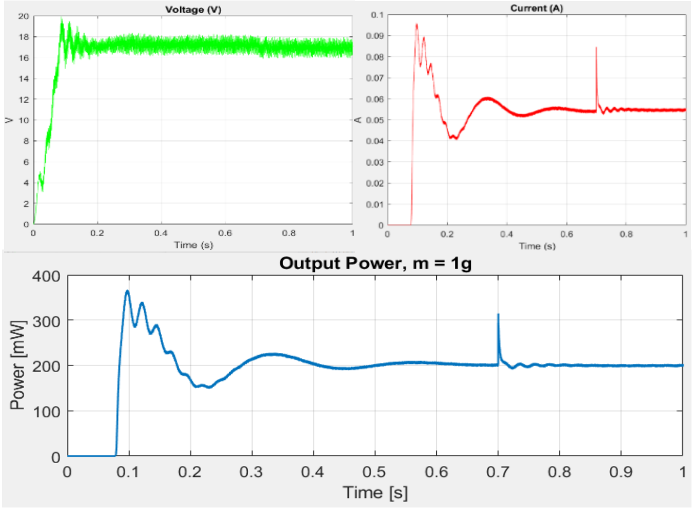

Fig. 6. Voltage, current and power recovered from a 1g mass.

Figure 6 shows the output voltage, the output current and the output power of the energy harvesting system, when the mass is equal to 1 g. These results are the best among the cases we have considered for comparison. The voltage can reach 18 V and the current is 0.055 A, which is an extremely significant value. The response is also faster than in the other cases, which can be attributed to the direct relationship between the mass and the resonance frequency, as demonstrated in equation (10).

3.2 Discussion

Figure 7 illustrate the power obtained from the three different masses at a frequency of 0.7 Hz. The energy recovered amounts to 25 mW for a mass of 1.2 g, 52 mW for a mass of 0.8 g and 196 mW for a mass of 1 g. These results clearly show that the mass has a significant impact on the performance of the energy recovery system. In particular, a mass of 1 g enhances recovered power, underlining the importance of choosing the right mass to maximize system efficiency. According to the recovered power results, mass plays a very important role in system performance by influencing the resonant frequency, as shown in equation (11). We now know that a mass of 1 g is the best option for our energy harvesting system, as it offers the highest recovered power among the values tested.
The power results obtained during simulations with the energy recovery system under three different cases of excitation frequency or walking further support this conclusion.

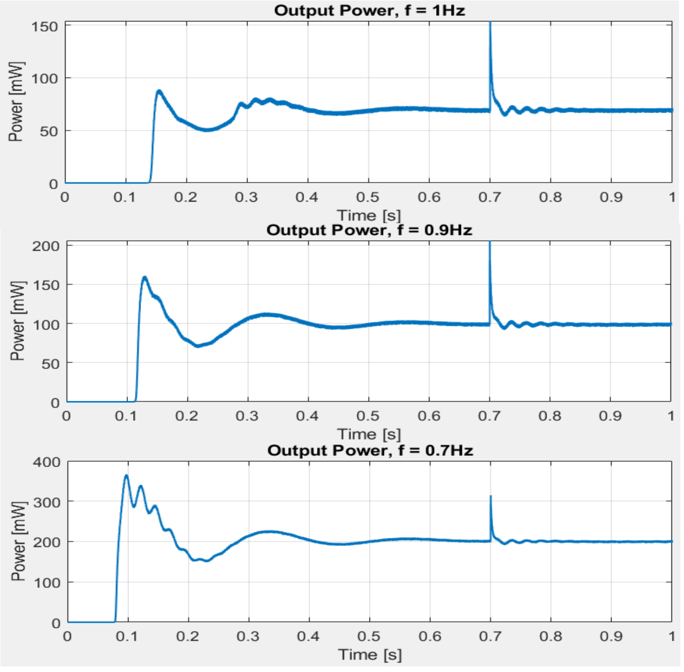

Fig. 7. Power recovery at different walking frequencies.

Figure 7 shows that the power at the 0.9 Hz frequency, with a value of 98 mW, is higher than that observed at the 1 Hz frequency, which is 68 mW, but lower than that measured at the 0.7 Hz operating frequency, which reaches 196 mW. This variation is explained by the increase in amplitude due to the decrease in frequency, in accordance with equation (10).
The simulation results agree with the theoretical study of motion amplitude. Each time the amplitude is increased, our system reacts efficiently and recovers more power. At this point, it is demonstrated that both the choice of the energy harvesting system's architecture and operating near the resonant frequency significantly influence the amount of energy recovered.

3.3 Electrical optimization

To improve the performance of the electronic energy harvesting system, the SSHI optimization method is used. The SSHI method's non-linear approach enables energy recovery and vibration control using piezoelectric elements. Synchronized Switch Harvesting on Inductor is a semi-passive technique designed to improve device efficiency by reversing the piezoelectric voltage at each deformation point [23].
To improve efficiency, the SSHI method reverses the piezoelectric voltage at each deformation point. Parallel and serial SSHI are two types of method that aim to invert the piezoelectric voltage in order to improve energy recovery efficiency. However, they differ in their practical application. The important distinction lies in the way the inductor is connected to the piezoelectric circuit. The performance, losses and complexity of the associated electronic circuit can be affected by this [23]. In addition to the SSHI approach, we also considered replacing the single diodes in the rectifier bridge with 1N5711 Schottky diodes. A metal-silicon junction diode, the 1N5711, is known for its high breakdown voltage, low threshold voltage and ultra-fast switching capability. In particular, it features a nominal reverse current of 200 nA. The main aim of this study is to minimize the current losses caused by its low resistance and the need to recharge the battery.

3.3.1 Parallel SSHI

In the parallel SSHI configuration, the inductor is connected in parallel with the piezoelectric elements.

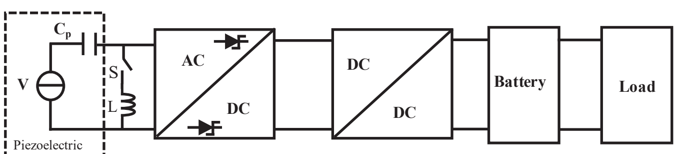

Fig. 8. P-SSHI interface circuit.

When the piezoelectric voltage reaches an extremum, the switch closes, creating an oscillating circuit between the inductance and the piezoelectric capacitance. This also inverts the piezoelectric voltage. The energy dissipated in the load resistor is the recovered power. It is represented by equation (11). For a resistor R_{opt} equation (12), the power admits a maximum P_{max} equation (13).

$$P = \frac{4\,\alpha^2 R}{(RC_p(1-\gamma)+\pi)^2}\,\omega^2\,u_M^2 \tag{11}$$

$$R_{opt} = \frac{\pi}{(1-\gamma)\omega\,C_p} \tag{12}$$

$$P_{max} = \frac{\alpha^2}{(1-\gamma)\,\pi\,C_p}\,\omega\,u_M^2 \tag{13}$$

Power recovery depends on the system frequency and the amplitude of the sinusoidal motion.

3.3.2 Serial SSHI

The SSHI series configuration involves connecting the inductor in series with the piezoelectric elements.

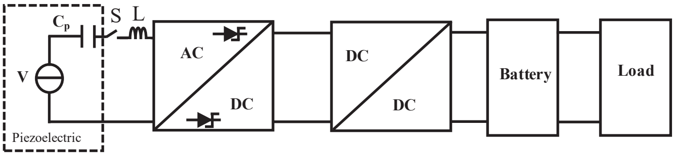

Fig. 9. S-SSHI interface circuit.

The switch closes when the piezoelectric voltage reaches a peak, generating an oscillating circuit between the inductance and the piezoelectric capacitance. This also reverses the piezoelectric voltage. The power delivered by the generator is given by equation (14) as a function of the load R, the amplitude of the exciting force and the model parameters α, γ inversion coefficient and C_p:

$$P = \frac{4\alpha^2 R (1+\gamma)^2}{(2 R C_p \omega(1+\gamma)+\pi(1-\gamma))^2} \omega^2 u_M^2 \qquad (14)$$

$$P_{max} = \frac{\alpha^2}{2 \pi C_p} \frac{(1+\gamma)}{(1-\gamma)} \omega \; u_M^2 \qquad (15)$$

$$R_{opt} = \frac{\pi}{2 \omega C_p} \frac{(1+\gamma)}{(1-\gamma)} \qquad (16)$$

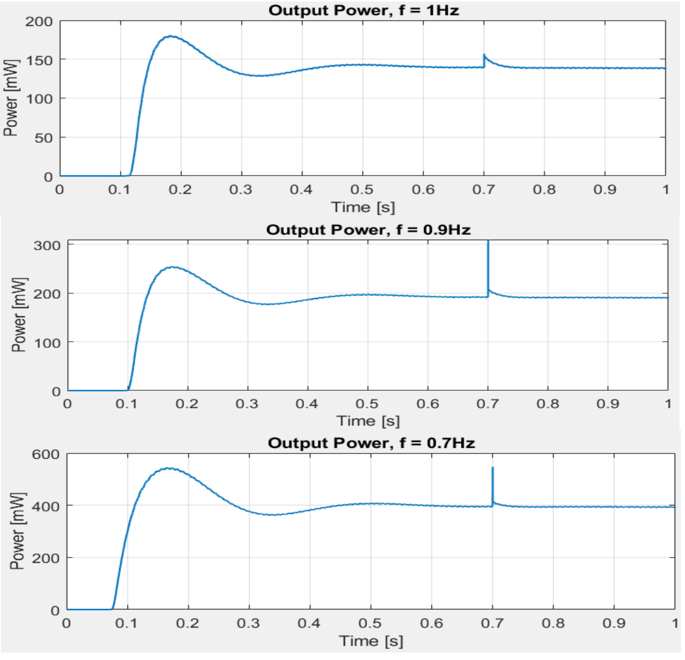

Fig. 10. Power recovery using the P-SSHI method.

The system frequency and the amplitude of the sinusoidal motion always condition the recovered power. After using the SSHI method, the simulation results focus exclusively on the recovered power curves.

Figure 10 presents the power results using the parallel SSHI method at frequencies of 1 Hz, 0.9 Hz, and 0.7 Hz. The average power recovered at each frequency is 137 mW, 189 mW, and 391 mW, respectively.

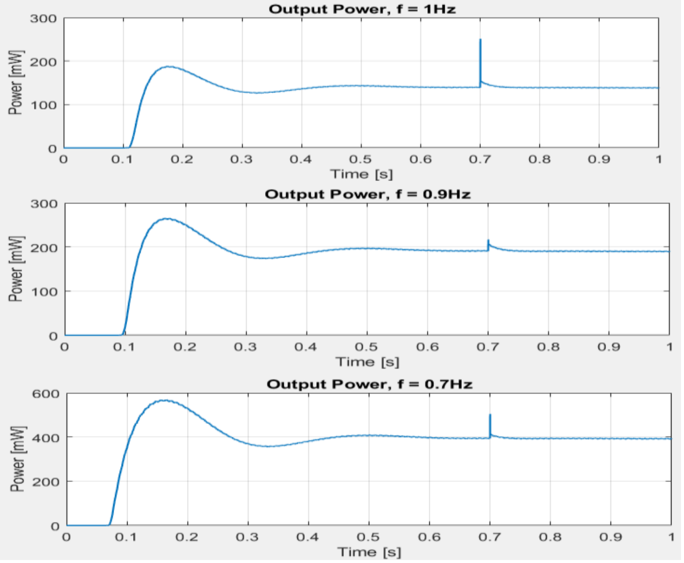

Fig. 11. Power recovery using the S-SSHI method.

The SSHI power series results at 0.9 Hz, are shown in Figure 11at frequencies of 1 Hz, 0.9 Hz, and 0.7 Hz. The average power recovered at each frequency is 139 mW, 190.30 mW, and 396 mW, respectively.

4 Discussions

Table 1. The power recovered during simulation.

Frequency (Hz)	Power(mw) with simple mounting	Power(mw) with P-SSHI + Schottky diodes	Power(mw) with S-SSHI +Schottky diodes
1	68	137	139
0.9	98	189	190.30
0.7	196	391	396

The improvement in results is remarkable, particularly in terms of the power recovered with the SSHI method and the new rectifier, compared with the first simple set-up. This clear improvement is attributed to two main factors. Firstly, the addition of switch S and coil L, i.e. SSHI methods, has optimized the power recovery process. Secondly, the replacement of single diodes with Schottky diodes played a crucial role. These diodes, characterized by low

reverse current, ensured more effective current response, thus promoting more efficient battery charging.
Simulation results show that the series SSHI method offers slightly better results than the parallel SSHI method. In fact, the series SSHI method enables the piezoelectric voltage to be inverted, thereby increasing the amplitude of the crenels and improving the efficiency of the device. This voltage inversion introduces a dry friction-type dissipative mechanism, resulting in frequency-independent losses, making this approach effective even at very low frequencies. In comparison, the parallel SSHI method does not offer the same advantages in terms of improved efficiency and reduced losses.
Table 2 summarizes the results obtained from the simulation of the proposed energy harvesting system. This system harnesses energy generated from human walking. These results validate the effectiveness of the proposed energy harvesting system in achieving increased efficiency.

5 Conclusion

In this paper, the energy Harvesting from very low excitation frequencies (0.7 Hz, 0.9 Hz, and 1.2 Hz), corresponding to humain walking, is investigated using a piezoelectric power device. The proposed generator is designed using a cantilever beam. During the optimization process, manual tuning of the concentrated mass at the end of the system was performed, adjusting its value to find the best configurations that enable the system to respond well and provide good results in terms of recovered power. For instance, with a mass of 1g and a motion frequency of 0.7 Hz, the power reached 196 mW, whereas with the same frequency but a mass of 1.2g, the power reached only 25 mW, with a longer delay for recovery. Consequently, the energy harvesting system was fixed with a mass of 1g for the remainder of the work.
Using this chosen model, the three cases of excitation frequency were analyzed to observe the variation of voltage and current as a function of frequency of excitation. At an excitation frequencies of 1 Hz, 0.9 Hz and 0.7 Hz the recovered power, at each frequency, reeached 68 mW, 98 mW and 196 mW respectively.
After selecting the model, efforts were directed towards enhancing the system to recover more power. Electrical improvements were made using the SSHI method, which inverts the piezoelectric voltage at each deformation point. Furthermore, simple diodes in the rectifier bridge were replaced with Schottky diodes, which have low reverse current, to maximize the current recovered by the piezoelectric device and improve power recovery results.
After these mechanical and electrical optimizations, simulation results showed that the recovered power reached up to 139 mW, 190.30 mW, and 396 mW. These results demonstrate the potential for further system improvements and the feasibility of developing a larger prototype capable of efficiently recovering and storing energy in batteries.

Acknowledgments

This research is on the frame of the APRD research program, Project REVPIEZO, funded by the Moroccan Ministry of Higher Education, Scientific Research and Innovation and the OCP Foundation.
This work was also carried out with the support of CNRST as part of the ''PhD-ASsociate Scholarship – PASS'' program.

References

Journal articles

1. Viet NV, Wang Q. Ocean wave energy pitching harvester with a frequency tuning capability. Energy 2018;162:603e17.
2. Gui P, Deng F, Liang Z, Cai Y, Chen J. Micro linear generator for harvesting mechanical energy from the human gait. Energy 2018;154:365e73.
3. Xin Y, Tian H, Guo C, Li X, Sun H, Wang P, Qian C, Wang S, Wang C. A biomimetic tactile sensing system based on polyvinylidene fluoride film. Rev Sci Instrum 2016;87(2):025002.
4. Kymissis J, Kendall C, Paradiso J, Gershenfeld N. In: Parasitic power harvesting in shoes 2nd IEEE Int. Conf. on wearable computers (cat. No. 98EX215); 1998. p. 132e9.
5. Tuncel, Yigit and Bandyopadhyay, Shiva and Kulshrestha, Shambhavi V. and Mendez, Audrey and Ogras, Umit Y. Towards wearable piezoelectric energy harvesting: modeling and experimental validation, 2020, 9781450370530.
6. Feng Qian, Tian-Bing Xu, Lei Zuo, Piezoelectric energy harvesting from human walking using a two-stage amplification mechanism, Energy, Volume 189, 2019, 116140, ISSN 0360-5442.
7. Almouahed S et al 2011 The use of piezoceramics as electrical energy harvesters within instrumented knee implant during walking IEEE-ASME T. Mech. 16 799–807.
8. Almouahed S, Hamitouche C and Stindel E 2016 Selfpowered device for tibiofemoral force measurement in knee implant 2016 2nd International Conference on Advanced Technologies for Signal and Image Processing (ATSIP) (IEEE).
9. Rocha J G et al 2010 Energy harvesting from piezoelectric materials fully integrated in footwear IEEE T. Ind. Electron. 57 813–9.
10. Shenck NS, Paradiso JA. Energy scavenging with shoe-mounted piezoelectrics. IEEE Micro 2001;21:30e42.
11. Qian F, Xu TB, Zuo L. Design, optimization, modeling and testing of a piezoelectric footwear energy harvester. Energy Convers Manag 2
12. Gonzalez J L, Rubio A and Moll F 2002 Human powered piezoelectric batteries to supply power to wearable electronic devices Int. J. Soc. of Mat. Eng. Resour. 10 34–40Z
13. L. Meirovitch, "Fundamentals of vibrations," New York: McGraw-Hill Book Co., 2001.
14. Shen D, Park JH, Noh JH, Choe SY, Kim SH, Wikle HC III, Kim DJ (2009) Micromachined PZT cantilever based on SOI structure for low frequency vibration energy harvesting. Sens Actuat A 154(1):103.
15. Yu H, Zhou J, Deng L, Wen Z (2014) A vibration-based MEMS piezoelectric energy harvester and power conditioning circuit. Sensors 14(2):3323.
16. Zhang G, Gao S, Liu H, Niu S (2017) A low frequency piezoelectric energy harvester with trapezoidal cantilever beam: theory and experiment. Microsystem Technologies 23(8):3457.
17. S. N. Chen, G. J. Wang, and M. C. Chien, "Analytical modeling of piezoelectric vibration-induced micro power generator," Mechatronics 16, 379– 387 (2006).
18. G. K. Ottman, H. F. Hofmann, A. C. Bhatt, and G. A. Lesieutre, "Adaptive piezoelectric energy harvesting circuit for wireless remote power supply," IEEE Transactions on Power Electronics 17, 669–676 (2002).
19. Ylli K, Hoffmann D, Willmann A, Becker P, Folkmer B, Manoli Y. Energy harvesting from human motion: exploiting swing and shock excitations. Smart Mater Struct 2015;24(2):025029.

20. Feng Qian and Tian-Bing Xu and Lei Zuo, Design, optimization, modeling and testing of a piezoelectric footwear energy harvester, Energy Conversion and Management, 2018, 0196-8904.
21. Thien Hoang. Dispositif de récupération d'énergie piézoélectrique : modélisation, fabrication et caractérisation. Electronique. Université de Tours, 2019. Français. ffNNT: ff. fftel-03216575ff.
22. Sylvain Drapier. Dynamics of Solids and Structures. École des Mines de Saint-Étienne. Saint-Étienne, France 2016
    https://www.emse.fr/~drapier/index_fichiers/CoursPDF/Dynamique-3A/Dynamique-SDrapier janvier2012.pdf)
23. Wu, Liao, Peidong Zhu, and Minghua Xie. 2021. "A Self-Powered Hybrid SSHI Circuit with a Wide Operation Range for Piezoelectric Energy Harvesting" *Sensors* 21, no. 2: 615. https://doi.org/10.3390/s21020615